

## Verification of the Re-Released ENDF/B VIII.0 Based Thermal Scattering Libraries

D. Kent Parsons\*, Cecile Toccoli†, and Jeremy L. Conlin†

\*Los Alamos National Laboratory, Los Alamos, NM 87544, [dkp@lanl.gov](mailto:dkp@lanl.gov)

†Los Alamos National Laboratory, Los Alamos, NM 87544, [ctoccoli@lanl.gov](mailto:ctoccoli@lanl.gov)

†Los Alamos National Laboratory, Los Alamos, NM 87544, [jlconlin@lanl.gov](mailto:jlconlin@lanl.gov)

### Introduction

An accurate description of the scattering of thermal neutrons ( $E < 4$  eV) is crucial for the design and safety of nuclear reactors, criticality safety, and shielding. The thermal scattering libraries (TSL) of evaluated nuclear data describe these low energy effects. ENDF/B-VIII.0 provides a major update to the ENDF thermal scattering library<sup>1,2</sup>. Indeed, it is nearly a completely new sub-library with 34 materials (with only 10 materials carried over from ENDF/B-VII.1) and many different temperatures for a total of 253 evaluated data files.

The first ACE formatted library released in 2018 by Los Alamos of this ENDF/B VIII.0 data was flawed, especially for TSL materials with incoherent thermal elastic scattering. Therefore, the thermal scattering evaluation files of the ENDF/B-VIII.0 library<sup>2</sup> have been recently re-processed at Los Alamos with NJOY2016<sup>3</sup>. This new library has been subjected to extensive verification testing:

- (1) continuity of scattering cross sections from the  $S(\alpha, \beta)$  to the free gas values,
- (2) consistency of the processed data and MCNP<sup>4</sup> test problem results with respect to material temperature,
- (3) comparison of ACER produced thermal cross sections with multi-group thermal cross sections from GROUPR.

### Thermal Scattering Law for Neutrons

When the neutron energy becomes comparable to the energy of the thermal motion of atoms within a material, neutrons become sensitive to binding effects. The cross sections evaluated from free-gas or free-atom models are no longer valid and should be replaced by thermal cross sections evaluated with Molecular Dynamics models.

Thermal cross sections are usually dominated by the incoherent inelastic scattering; the neutron exchanges energy (down- and up-scattered) with the target molecule or crystalline lattice and all the

scattered waves are assumed to combine incoherently without interference effects.

This incoherent inelastic thermal cross section  $\sigma^{\text{inc}}$  is described in terms of a bound cross section  $\sigma_b$  and a scattering function  $S(\alpha, \beta)$ <sup>5</sup>, where  $\alpha$  and  $\beta$  are reduced values for momentum transfer and energy transfer, respectively:

$$\sigma^{\text{inc}}(E, E' \mu) = \frac{\sigma_b}{2kT} \sqrt{\frac{E'}{E}} e^{-\frac{\beta}{2} S(\alpha, \beta)} \quad (1)$$

$$\text{with } \sigma_b = \sigma_f \frac{(A+1)^2}{A^2}, \quad (2)$$

$$\alpha = \frac{E' + E - 2\mu\sqrt{EE'}}{AkT} \text{ and } \beta = \frac{E' - E}{kT}, \quad (3), (4)$$

and where  $E$  and  $E'$  are the incident and scattered neutron energies,  $\mu$  is the cosine of the lab scattering angle,  $A$  the ratio of the target mass to the neutron mass;  $T$  is temperature and  $k$  the Boltzmann constant.

For a gas of particles with no internal structure (free-gas), the scattering function inferred in the free-gas cross section  $\sigma_f$  and is simply given by

$$S(\alpha, \beta) = \frac{1}{\sqrt{4\pi\alpha}} \exp\left\{-\frac{\alpha^2 + \beta^2}{4\alpha}\right\} \quad (5)$$

With increasing energy, neutrons become less sensitive to thermal scattering effects. The thermal  $S(\alpha, \beta)$  scattering data should asymptote into the free-gas scattering data at and near the transition energy denoted as  $E_{\text{max}}$  in ENDF/B formats and NJOY.  $E_{\text{max}}$  typically occurs between 1 and 10 eV neutron incident energy.

### Continuity of Scattering Cross Sections at $E_{\text{max}}$

Good  $S(\alpha, \beta)$  data will therefore have:

- Asymptotic behavior that reflects the lessening of low energy effects in the  $S(\alpha, \beta)$  data as the neutron energy approaches  $E_{\text{max}}$
- Consistency between the thermal and free-gas cross sections where the two models “connect” at

$E_{\max}$ . Any significant discontinuity in the scattering cross sections will adversely impact neutron transport calculations.

Figure 1 shows the total thermal neutron cross sections for a bound hydrogen atom in 6 different materials that asymptote into the underlying free-gas neutron cross section for H from ENDF/B-VIII.0. Ideally, the  $S(\alpha, \beta)$  and free-gas cross sections should match perfectly at  $E_{\max}$ . However, the thermal cross section does not always exactly equal the free-gas cross section. The observed discrepancies reflect the different origins of the data<sup>6</sup>. As long as the discrepancies are “small”, the  $S(\alpha, \beta)$  data is considered to be acceptable.

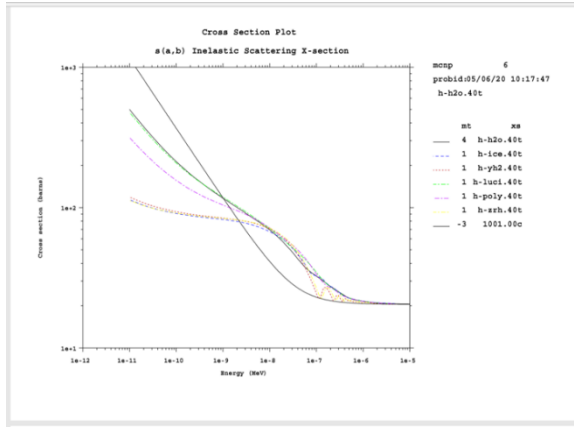


**Fig. 1. Thermal cross sections for bound hydrogen from six materials at room temperature.**

#### Thermal Cross Section Consistency with Respect to Temperature

The knowledge of the thermal cross sections at higher temperature is essential for “real-life” simulations. With increasing temperatures, the motion of atoms in molecule or crystal as well as the motion of the molecules and crystal increases. Consequently, the thermal cross section, governed by the inelastic incoherent component, is higher for increasing temperatures and the most significant relative increase is located at lowest energies. This expected behavior is seen on the Figure 2 that plots the thermal cross sections of bound H in ZrH for eight temperatures.

A simple infinite medium MCNP test problem has also been developed for each material at each temperature for both scattering treatments. These 506 test problems have been run and MCNP edit

outputs (number of collisions, mean free path, average neutron velocity, and neutron lifetime) with respect to the temperature or other properties have been observed and recorded. Valuable insights into thermal neutron scattering can be deduced from these results. See the companion summary<sup>8</sup> to this paper. A pair of sample tables (see Tables I and II) of MCNP test problem results are given below for 1.6 g/cc reactor graphite with 10% porosity.

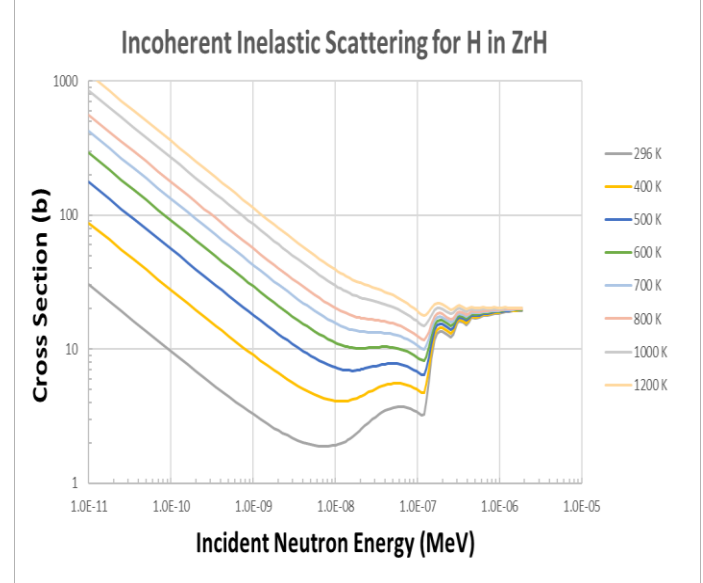


**Fig. 2. Thermal cross sections for bound hydrogen in ZrH for eight temperatures.**

**Table I. Test Problem Results for  $S(\alpha, \beta)$  10% Porosity Reactor Graphite**

temp (K)	avg. no. collisions	lifetime (sh)	mfp (cm)	avg n vel (m/sec)
296	1412.4	1.173E+06	2.1149	2494
400	1653.9	1.173E+06	2.0697	2899
500	1854.7	1.172E+06	2.0543	3241
600	2036.5	1.172E+06	2.0472	3551
700	2202.7	1.172E+06	2.0433	3835
800	2357.6	1.173E+06	2.0408	4099
1000	2640.1	1.173E+06	2.0379	4583
1200	2894.4	1.172E+06	2.0360	5021
1600	3348.6	1.173E+06	2.0333	5797
2000	3748.6	1.173E+06	2.0317	6482

**Table II. Test Problem Results for free gas 10% Porosity Reactor Graphite**

temp (K)	avg. no. collisions	lifetime (sh)	mfp (cm)	avg n vel (m/sec)
296	1450.4	1.172E+06	2.0199	2493
400	1687.0	1.173E+06	2.0195	2898
500	1885.8	1.173E+06	2.0196	3240
600	2065.6	1.173E+06	2.0197	3549
700	2231.2	1.173E+06	2.0198	3833
800	2385.5	1.173E+06	2.0198	4098
1000	2666.4	1.174E+06	2.0201	4581
1200	2921.0	1.173E+06	2.0200	5019
1600	3372.6	1.172E+06	2.0201	5796
2000	3770.3	1.173E+06	2.0201	6478

Note that implicit capture was not used in MCNP for these test problems so that the number of collisions does correspond to the actual number of collisions. Also, the number of collisions only includes collisions at thermal conditions since the initial fixed neutron source was set to a Maxwellian distribution at the material temperature. Finally, the neutron velocity at room temperature is not the well-known 2200 m/sec most likely velocity, but rather the true average velocity.

The neutron lifetimes shown in the tables above correspond to the thermal diffusion time and are independent of material temperature and scattering treatment. The lifetime is only dependent on the average neutron velocity and the capture cross section (with its 1/v energy dependence).

### Continuous and Multi-Group Thermal Cross Section Comparisons

Another verification of the new ACE sub-libraries has been made by comparing continuous energy cross sections in the ACE formatted files with multi-group cross sections from the GROUPR module of NJOY. The multi-group thermal data are generated from the same sequence of NJOY processing until after the THERMR module. The part of the TSL processing done in ACER along with the user input to ACER can thus be compared with the processing done in GROUPR along with the user input to GROUPR.

GROUPR is run with a smooth weighting function with an arbitrary energy grid chosen to give

a reasonable number of groups in the thermal energy range.

Agreement between continuous and multi-group thermal scattering cross sections has been demonstrated for all three existing types of TSL files in the library:

- Inelastic scattering only (e.g. light water),
- Inelastic and coherent elastic scattering (e.g., graphite),
- Inelastic and incoherent elastic scattering (e.g., bound H in ZrH).

Figures 3, 4, and 5 illustrate these results. Light water at room temperature is shown in Figure 3 and reactor graphite with 10% porosity at 400 K is shown in Figure 4. H in ZrH at 500 k is shown in Figure 5. In all cases, multi-group cross sections are shown in a “stairstep” curve.

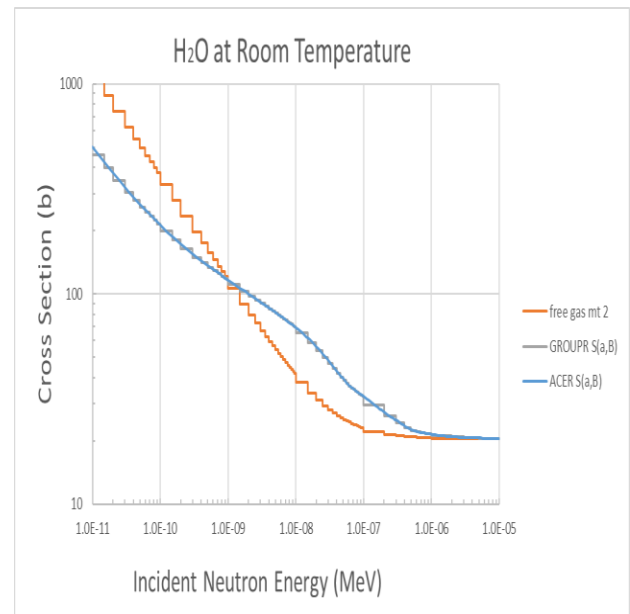


**Fig. 3. Comparison of ACER and GROUPR scattering cross sections for H in room temperature H<sub>2</sub>O.**

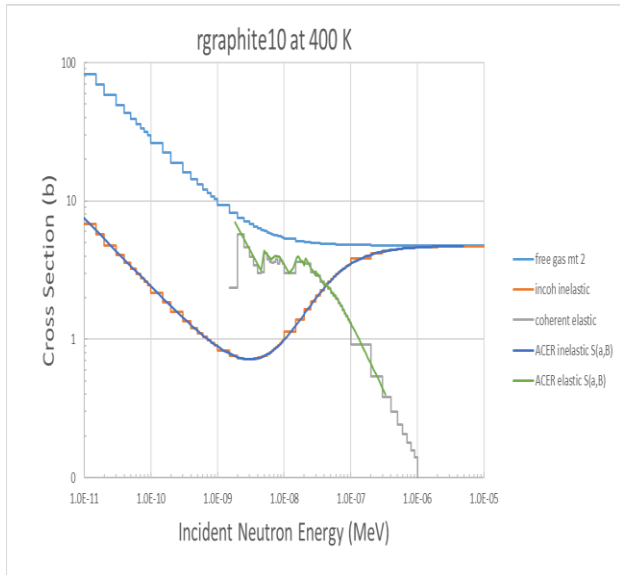


**Fig. 4, Comparison of ACER and GROUPR scattering cross sections for reactor graphite with 10% porosity at 400 K.**

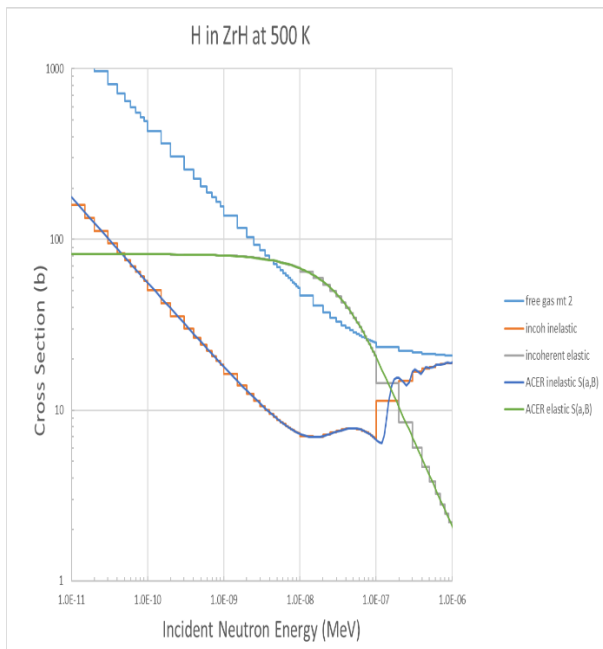


**Fig. 5, Comparison of ACER and GROUPR scattering cross sections for H in ZrH at 500 K**

## Summary

In the course of re-processing the ENDF/B VIII.0 thermal scattering files, three verification methods have been implemented at Los Alamos. These methods give reasonable assurance that the re-processed ACE files with thermal scattering data are correct.

The verification tests presented in this paper constitute a first step of a more comprehensive validation procedure for the thermal sub-libraries at LANL. Contemplated additional tests for the future includes work on the differential in energy and angle scattering laws, comparisons with non-LANL nuclear data processing codes, and possibly comparisons with experiments.

## References:

1. D.A. Brown, "README.txt" documentation file supplied with the thermal scattering data of ENDF/B-VIII.0, National Nuclear Data Center, (2018).
2. D.A. Brown, *et al.* "ENDF/B-VIII.0: The 8th Major Release of the Nuclear Reaction Data Library with CIELO-project Cross sections, New Standards and Thermal Scattering Data," Nuclear Data Sheets 148, 1 (2018).
3. R. MacFarlane *et al.*, The NJOY Nuclear Data processing system, version 2016, Technical report (2017).
4. C.J. Werner (editor), "MCNP Users Manual – Code Version 6.2", report LA-UR-29981 (2017).
5. G.L. Squires, Introduction to the Theory of Thermal Neutron Scattering 3<sup>rd</sup> edn, Cambridge University Press (2002).
6. V.F. Sers, Neutron scattering lengths and cross sections, Neutron News, 3:3, 26-37 (1992).
7. D.K. Parsons and C. Toccoli, "Re-Release of the ENDF/B VIII.0 S(α,β) Data Processed by NJOY2016", LA-UR-20-nnnnn, online documentation found with the thermal scattering sub-libraries at <http://nucleardata.lanl.gov>, Los Alamos National Laboratory, (2020).
8. K. Parsons and C. Toccoli, "Analytic Insights into the Neutronic Characteristics of Neutron Moderators from MCNP Calculations", this conference.